

THE ANALOG BOUNDARY INTEGRAL EQUATION METHOD FOR NONLINEAR STATIC AND DYNAMIC PROBLEMS IN CONTINUUM MECHANICS

JOHN T. KATSIKADELIS

Department of Civil Engineering, National Technical University of Athens, Greece
e-mail: jkats@central.ntua.gr

In this paper the Analog Equation Method (AEM), a boundary-only method, is presented for solving nonlinear static and dynamic problems in continuum mechanics. General bodies are considered, that is bodies whose properties may be position or direction dependent and their response is nonlinear. The nonlinearity may result from both nonlinear constitutive relations (material nonlinearity) and large deflections (geometrical nonlinearity). The quintessence of the method is the replacement of the coupled nonlinear partial differential equations with variable coefficients governing the response of the body by an equivalent set of linear uncoupled equations under fictitious sources. The fictitious sources are established using a BEM-based technique and the solution to the original problem is obtained from the integral representation of the solution to the substitute problem. A variety of static and dynamic problems solved using the AEM are presented to illustrate the method and demonstrate its efficiency and accuracy.

Key words: continuum mechanics, general bodies, boundary elements, analog equation, integral equation method

1. Introduction

Boundary methods are known for their major advantage to restrict the discretization only to the boundary of a body. Among them, the most reputed one is the boundary integral equation or otherwise known as Boundary Element Method (BEM), a name resulting from the employed technique to solve boundary integral equations. Although the BEM has been proven to be a powerful alternative to the so called domain methods, such as FDM and FEM, when linear problems are encountered, this method has been criticized

as in capable of solving nonlinear problems, especially in nonhomogeneous bodies where coefficients of differential equations are variable. This is one of the reasons that many investigators are reluctant to be involved with BEM and use it as a computational tool.

The effort to develop BEM methods for nonlinear problems has been given by many BEM investigators. Almost all of these methods have not avoided the domain discretization. The only method that can be considered as boundary-only is the Dual Reciprocity Method (DRM) (Patridge et al., 1992). The term *boundary-only* is used in the sense that the discretization and integration are limited only on the boundary, although collocation points inside the domain may be used to improve the solution. Nevertheless, DRM works when for a non standard linear partial differential equation or a nonlinear one it is possible to extract a standard linear partial differential operator $L(\cdot)$ and lump the remainder together in the right-hand-side as a body-force term

$$L(u) = b(x, y, u, u_x, u_y, u_{xx}, u_{xy}, u_{yy}) \quad (1.1)$$

where $b(\cdot)$ is, in general, a nonlinear function of its arguments.

Further, DRM can be employed if the fundamental solution to the adjoint differential equation can be established, namely, a partial singular solution to the equation

$$L^*(u^*) = \delta(P - Q) \quad (1.2)$$

where $L^*(\cdot)$ is the adjoint operator to $L(\cdot)$ and $\delta(P - Q)$ is the Dirac delta function.

On the basis of the aforementioned, it is apparent that DRM cannot be employed when:

(a) the differential operator cannot be put in the form of Eq. (1.1), e.g.

$$u_{xx}u_{yy} - u_{xy}^2 = f(x, y) \quad (1.3)$$

(b) the fundamental solution to Eq. (1.2) is not available, e.g. when the operator $L^*(\cdot)$ has variable coefficients.

Apparently, the efficiency of DRM decreases in the case of problems described by coupled nonlinear equations. Besides, different DRM formulations, and consequently, different computer programs are required for different body force terms as well as for different operators $L^*(\cdot)$, even when the order of the equations is the same.

In this paper a boundary-only method is presented for solving nonlinear static and dynamic problems. The method alleviates the restrictions characterizing DRM. Simple fundamental solutions are used in it, which depend only

on the order of differential equations, e.g. for second order differential equations the fundamental solution to the Laplace equation is employed for both static and dynamic problems. The method is based on the concept of the analog equation (Katsikadelis, 1994b), according to which a nonlinear problem is replaced by an equivalent simple linear one under a fictitious source with the same boundary and initial conditions. The substitute problem is chosen so that the integral representation of the solution is known. The fictitious source is established by approximating it with a radial basis function series expansion as in DRM and the solution to the original problem is computed from the integral representation of the substitute problem, which is used as a mathematical formula. Without restricting the generality, the method is illustrated by applying it to second and fourth order partial differential equations.

The method has been already successfully employed to solve a variety of engineering problems described by partial differential equations, among them potential flow problems in bodies whose material constants depend on the field function (e.g. temperature dependent conductivity) (Katsikadelis and Nerantzaki, 1999b), determination of surface with prescribed mean or total curvature (Katsikadelis and Nerantzaki, 1999b), the soap bubble problem (Katsikadelis and Nerantzaki, 2001), nonlinear static and dynamic analysis of homogeneous isotropic and heterogeneous orthotropic membranes (Katsikadelis et al., 2001; Katsikadelis, 2002; Katsikadelis and Tsiatas, 2001b,c), finite elasticity problems, inverse problems (Nerantzaki and Katsikadelis, 1998), equationless problems in nonlinear bodies using only boundary data (Katsikadelis and Nerantzaki, 1999a), nonlinear analysis of shells (Yiotis and Katsikadelis, 2001). The method has been also applied to problems described by coupled nonlinear ordinary differential equations, e.g. finite deformation analysis of elastic cables (Katsikadelis and Apostolopoulos, 1995; Katsikadelis, 2001), large deflection analysis of beams (Katsikadelis and Tsiatas, 2001a) and integration of nonlinear equations of motion (Katsikadelis, 1994a). Some exemplary problems are solved to demonstrate the applicability, efficiency and accuracy of AEM.

2. Illustration of AEM for 2nd order PDEs of hyperbolic type

2.1. Problem statement

Consider a non-homogeneous body occupying the two-dimensional domain Ω in the xy -plane (Fig. 1), whose dynamic response is governed by the following initial boundary value problem

$$\begin{aligned}
 \rho u_{tt} + cu_t + N(u) &= g(x, y, t) && \text{in } \Omega, \quad 0 \leq t \\
 \beta_1 u + \beta_2 u_n &= \beta_3 && \text{on } \Gamma \\
 \left. \begin{aligned} u(x, y, 0) &= u_1(x, y) \\ u_t(x, y, 0) &= u_2(x, y) \end{aligned} \right\} && \text{in } \Omega
 \end{aligned} \tag{2.1}$$

where $u = u(x, y, t)$ is the unknown field function and

$$N(u) = N(u, u_x, u_y, u_{xx}, u_{xy}, u_{yy}, x, y) \tag{2.2}$$

is a nonlinear second order differential operator defined in Ω ; $\Gamma = \bigcup_{i=0}^{i=K} \Gamma_i$ is the boundary where Γ_i ($i = 1, 2, \dots, K$) are K non-intersecting closed contours surrounded by the contour Γ_0 . Moreover, $\beta_i = \beta_i(s)$, $i = 1, 2, 3$ are functions specified on the boundary Γ with s being the arc length, while $u_1(x, y)$ and $u_2(x, y)$ are given functions denoting the initial deflection and velocity distributions, respectively. Finally, $\rho = \rho(x, y)$ and $c = c(x, y)$ are the mass and damping densities, respectively, and $g(x, y, t)$ is the forcing function. Boundary condition (2.1)₂ is assumed linear for convenience in presenting the method, although a nonlinear boundary condition could be considered.

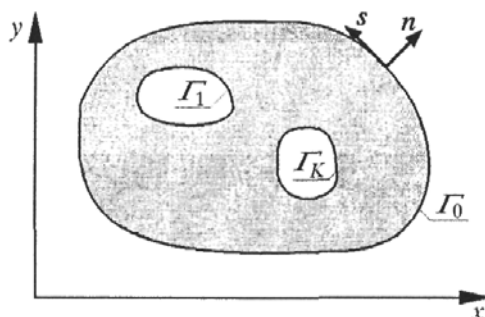


Fig. 1. Multiply connected domain Ω and boundary $\Gamma = \bigcup_{i=0}^{i=K} \Gamma_i$

2.2. The analog equation method

Let $u = u(x, y, t)$ be the sought solution to problem (2.1). This function is two times continuously differentiable in Ω . Thus, if the Laplace operator $\nabla^2 = \partial^2/\partial x^2 + \partial^2/\partial y^2$ is applied to it, we have

$$\nabla^2 u = b(x, y, t) \tag{2.3}$$

Eq. (2.3) is a quasi-static equation and indicates that the solution to Eq. (2.1)₁ at the instant t could be established by solving this equation under boundary

condition (2.1)₂, if the fictitious time dependent source $b(x, y, t)$ were known. Eq. (2.3) is *the analog equation*, which together with boundary condition (2.1)₂ and initial conditions (2.1)₃ constitute the substitute problem.

The fictitious source can be established following a procedure similar to that presented by Katsikadelis and Nerantzaki (1999b) for the static problem. We assume

$$b = \sum_{j=1}^M a_j f_j \tag{2.4}$$

where $f_j = f_j(x, y)$ is a set of approximation functions and $a_j = a_j(t)$ time dependent coefficients to be determined.

The solution to Eq. (2.3) at the instant t can be written as a sum of the homogeneous solution $\bar{u} = \bar{u}(x, y, t)$ and a particular solution $u_p = u_p(x, y, t)$ to the nonhomogeneous equation. Thus, we can write

$$u = \bar{u} + u_p \tag{2.5}$$

The particular solution is obtained from

$$\nabla^2 u_p = \sum_{j=1}^M a_j f_j \tag{2.6}$$

which yields

$$u_p = \sum_{j=1}^M a_j \hat{u}_j \tag{2.7}$$

where \hat{u}_j ($j = 1, 2, \dots, M$) is a particular solution to the equation

$$\nabla^2 \hat{u}_j = f_j \quad j = 1, 2, \dots, M \tag{2.8}$$

The particular solution to Eq. (2.8) can always be determined, if f_j is specified. The homogeneous solution \bar{u} is obtained from the boundary value problem

$$\begin{aligned} \nabla^2 \bar{u} &= 0 && \text{in } \Omega \\ \beta_1 \bar{u} + \beta_2 \bar{q} &= \beta_3 - \left(\beta_1 \sum_{j=1}^M a_j \hat{u}_j + \beta_2 \sum_{j=1}^M a_j \hat{q}_j \right) && \text{on } \Gamma \end{aligned} \tag{2.9}$$

where $\hat{q}_j = \partial \hat{u}_j / \partial n$.

Boundary value problem (2.9) is solved using BEM. Thus, the integral representation of the solution \bar{u} is given as

$$c\bar{u}(P, t) = - \int_{\Gamma} (u^* \bar{q} - \bar{u} q^*) ds \quad P\{x, y\} \in \Omega \cup \Gamma \tag{2.10}$$

in which $u^* = \ln(r/2\pi)$ is the fundamental solution to Eq. (2.9)₁ and $q^* = u_{,n}^*$ its derivative normal to the boundary with $r = |Q-P| = \sqrt{(\xi-x)^2 + (y-\eta)^2}$ being the distance between any two points $P(x,y)$ in $\Omega \cup \Gamma$, $Q(\xi,\eta)$ on Γ ; c is a constant which takes the values $c = 1$ if $P \in \Omega$ and $c = \alpha/2\pi$ if $P \in \Gamma$; α is the interior angle between the tangents of the boundary at the point P . Note, that it is $c = 1/2$ for points where the boundary is smooth.

On the basis of Eqs (2.5), (2.7) and (2.10), the solution to Eq. (2.3) is written as

$$cu = - \int_{\Gamma} (u^* \bar{q} - \bar{u} q^*) ds + \sum_{j=1}^M a_j \hat{u}_j \tag{2.11}$$

Differentiating the above equation for $P \in \Omega$ ($c = 1$) yields

$$\begin{aligned} u_x &= - \int_{\Gamma} (u_x^* \bar{q} - \bar{u} q_x^*) ds + \sum_{j=1}^M (\hat{u}_j)_x a_j \\ u_y &= - \int_{\Gamma} (u_y^* \bar{q} - \bar{u} q_y^*) ds + \sum_{j=1}^M (\hat{u}_j)_y a_j \\ u_{yy} &= - \int_{\Gamma} (u_{xx}^* \bar{q} - \bar{u} q_{xx}^*) ds + \sum_{j=1}^M (\hat{u}_j)_{xx} a_j \\ u_{xx} &= - \int_{\Gamma} (u_{yy}^* \bar{q} - \bar{u} q_{yy}^*) ds + \sum_{j=1}^M (\hat{u}_j)_{yy} a_j \\ u_{xy} &= - \int_{\Gamma} (u_{xy}^* \bar{q} - \bar{u} q_{xy}^*) ds + \sum_{j=1}^M (\hat{u}_j)_{xy} a_j \end{aligned} \tag{2.12}$$

The final step of AEM is to apply Eq. (2.1)₁ to M discrete points inside Ω . Thus, we obtain a set of M equations

$$\rho^i u_{tt}^i + c^i u_t^i + N(u^i) = g^i \quad i = 1, 2, \dots, M \tag{2.13}$$

Using Eqs (2.11) and (2.12) to evaluate u and its derivatives at the points $i = 1, 2, \dots, M$ and substituting them into Eq. (2.13), the following set of nonlinear ordinary differential equations, which play the role of the semidiscretized equations of motion, is obtained

$$F_i(a_j, \dot{a}_j, \ddot{a}_j) = g^i \quad i = 1, 2, \dots, M \tag{2.14}$$

which can be solved to yield the coefficients a_j . The AEM can be implemented only numerically.

2.3. Numerical implementation

The BEM with constant elements is used to approximate the boundary integrals in Eqs (2.11) and (2.12). If N is the number of the boundary nodal points (see Fig. 2), then Eq. (2.11) is written as

$$c^i \bar{u}^i = \sum_{k=1}^N \tilde{H}_{ik} \bar{u}^k - \sum_{k=1}^N G_{ik} \bar{q}^k \tag{2.15}$$

where

$$\tilde{H}_{ik} = \int_k q^*(r_{ik}) ds \qquad G_{ik} = \int_k u^*(r_{ik}) ds \tag{2.16}$$

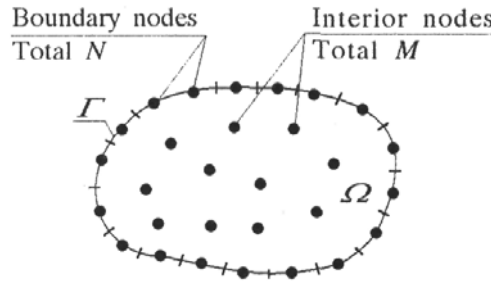


Fig. 2. Boundary discretization and domain nodal points

Applying Eq. (2.15) to all boundary nodal points and using matrix notation yields

$$\mathbf{H}\bar{\mathbf{u}} - \mathbf{G}\bar{\mathbf{q}} = \mathbf{0} \tag{2.17}$$

where

$$\mathbf{H} = \tilde{\mathbf{H}} - \mathbf{C} \tag{2.18}$$

with \mathbf{C} being a diagonal matrix including values of the coefficient c^i . Boundary condition (2.9)₂, when applied to the N boundary nodal points, yields

$$(\beta_1)^i \bar{u}^i + (\beta_2)^i \bar{q}^i = (\beta_3)_i - \left[(\beta_1)^i \sum_{j=1}^M a_j \hat{u}_j^i + (\beta_2)^i \sum_{j=1}^M a_j \hat{q}_j^i \right] \tag{2.19}$$

or using the matrix notation

$$\beta_1 \bar{\mathbf{u}} + \beta_2 \bar{\mathbf{q}} = \beta_3 - (\beta_1 \hat{\mathbf{U}} + \beta_2 \hat{\mathbf{Q}}) \mathbf{a} \tag{2.20}$$

in which $\hat{\mathbf{U}} = \hat{\mathbf{u}}_j^i$, $\hat{\mathbf{Q}} = \hat{\mathbf{q}}_j^i$ are $N \times M$ known matrices; β_1, β_2 are $N \times N$ known diagonal matrices, and \mathbf{a} is the vector of the coefficients to be determined.

Eqs (2.17) and (29) may be combined to express \bar{u} and \bar{q} in terms of \mathbf{a} . Thus, we may write

$$\begin{bmatrix} \mathbf{H} & -\mathbf{G} \\ \beta_1 & \beta_2 \end{bmatrix} \begin{Bmatrix} \bar{u} \\ \bar{q} \end{Bmatrix} = \begin{bmatrix} \mathbf{0} \\ \mathbf{T} \end{bmatrix} \mathbf{a} + \begin{Bmatrix} \mathbf{0} \\ \beta_3 \end{Bmatrix} \tag{2.21}$$

where

$$\mathbf{T} = -(\beta_1 \hat{\mathbf{U}} + \beta_2 \hat{\mathbf{Q}}) \tag{2.22}$$

Solving Eq. (2.21), yields

$$\bar{u} = \mathbf{S}_u \mathbf{a} + \mathbf{d}_u \qquad \bar{q} = \mathbf{S}_q \mathbf{a} + \mathbf{d}_q \tag{2.23}$$

in which $\mathbf{S}_u, \mathbf{S}_q$ are known $N \times M$ rectangular matrices and $\mathbf{d}_u, \mathbf{d}_q$ known vectors. Eqs (2.11) and (2.12), when discretized and applied to the M nodal points inside Ω , give

$$\begin{aligned} \mathbf{u} &= \mathbf{H}\bar{u} - \mathbf{G}\bar{q} + \hat{\mathbf{U}}\mathbf{a} \\ \mathbf{u}_x &= \mathbf{H}_x\bar{u} - \mathbf{G}_x\bar{q} + \hat{\mathbf{H}}_x\mathbf{a} \\ \mathbf{u}_y &= \mathbf{H}_y\bar{u} - \mathbf{G}_y\bar{q} + \hat{\mathbf{U}}_y\mathbf{a} \\ \mathbf{u}_{xx} &= \mathbf{H}_{xx}\bar{u} - \mathbf{G}_{xx}\bar{q} + \hat{\mathbf{U}}_{xx}\mathbf{a} \\ \mathbf{u}_{yy} &= \mathbf{H}_{yy}\bar{u} - \mathbf{G}_{yy}\bar{q} + \hat{\mathbf{U}}_{yy}\mathbf{a} \\ \mathbf{u}_{xy} &= \mathbf{H}_{xy}\bar{u} - \mathbf{G}_{xy}\bar{q} + \hat{\mathbf{U}}_{xy}\mathbf{a} \end{aligned} \tag{2.24}$$

in which $\mathbf{G}, \mathbf{H}, \mathbf{G}_x, \mathbf{H}_{yy}, \dots, \mathbf{H}_{xy}$ are known $M \times M$ matrices originating from the integration of the kernel functions u^* and q^* and their respective derivatives; $\hat{\mathbf{U}}, \hat{\mathbf{H}}_x, \dots, \hat{\mathbf{U}}_{xy}$ are known matrices having dimensions $M \times M$, the elements of which result from the functions \hat{u}_j and their derivatives.

Substituting Eqs (2.23) into Eqs (2.24), yields

$$\begin{aligned} \mathbf{u} &= \mathbf{W}\mathbf{a} + \mathbf{w} \\ \mathbf{u}_x &= \mathbf{W}_x\mathbf{a} + \mathbf{w}_x \qquad \mathbf{u}_y = \mathbf{W}_y\mathbf{a} + \mathbf{w}_y \\ \mathbf{u}_{xx} &= \mathbf{W}_{xx}\mathbf{a} + \mathbf{w}_{xx} \qquad \mathbf{u}_{yy} = \mathbf{W}_{yy}\mathbf{a} + \mathbf{w}_{yy} \\ \mathbf{u}_{xy} &= \mathbf{W}_{xy}\mathbf{a} + \mathbf{w}_{xy} \end{aligned} \tag{2.25}$$

where $\mathbf{W}, \mathbf{W}_x, \dots, \mathbf{W}_{xy}$ are known matrices and $\mathbf{w}, \mathbf{w}_x, \dots, \mathbf{w}_{xy}$ known vectors.

Differentiating Eq. (2.25)₁ with respect to time and taking into account that the vector \mathbf{w} is constant, we obtain

$$\dot{\mathbf{u}} = \mathbf{W}\dot{\mathbf{a}} \quad \ddot{\mathbf{u}} = \mathbf{W}\ddot{\mathbf{a}} \quad (2.26)$$

Finally, writing Eq. (2.13) in a matrix form and substituting Eqs (2.25) and (2.26) in it, we obtain the typical semidiscretized nonlinear equation of motion

$$\mathbf{M}\ddot{\mathbf{a}} + \mathbf{C}\dot{\mathbf{a}} + \mathbf{N}(\mathbf{a}) = \mathbf{g} \quad (2.27)$$

where \mathbf{M} and \mathbf{C} are generalized mass and damping matrices, respectively. The initial conditions for Eq. (2.27) are obtained from Eqs (2.25)₁ and (2.26)₁ on the basis of Eqs (2.1)₃. Thus, we have

$$\mathbf{a}(0) = \mathbf{W}^{-1}(\mathbf{u}_1 - \mathbf{w}) \quad \dot{\mathbf{a}}(0) = \mathbf{W}^{-1}\mathbf{u}_2 \quad (2.28)$$

2.3.1. The dynamic problem

For forced ($g(x, y, t) \neq 0$) or free vibrations ($g(x, y, t) = 0$), Eq. (2.27) is solved using any time step integration method taking into account initial conditions (2.28). Once a_j are computed, the solution to the problem and its derivatives are evaluated from Eqs (2.25). For points not coinciding with the nodal points, these quantities are computed from the discretized counterpart of Eqs (2.11) and (2.12).

2.3.2. The static problem

In this case it is $\dot{\mathbf{a}} = \ddot{\mathbf{a}} = \mathbf{0}$, and Eq. (2.27) becomes

$$\mathbf{N}(\mathbf{a}) = \mathbf{g} \quad (2.29)$$

from which the coefficients \mathbf{a} are established by solving a system of nonlinear algebraic equations.

3. Examples

On the basis of the numerical procedure presented in Section 2, a FORTRAN code has been written and numerical results for exemplary problems have been obtained, which illustrate the applicability, effectiveness and

accuracy of the AEM. The employed approximation functions f_j are the multiquadrics, which are defined as

$$f_j = \sqrt{r^2 + c^2} \tag{3.1}$$

where c is an arbitrary constant and

$$r = \sqrt{(x - x_j)^2 + (y - y_j)^2} \quad j = 1, 2, \dots, M \tag{3.2}$$

with x_j, y_j being the collocation nodal points inside Ω . Using these radial basis functions, the particular solution to Eq. (2.8) is obtained as

$$\hat{u}_j = -\frac{c^3}{3} \ln(c\sqrt{r^2 + c^2} + c^2) + \frac{1}{9}(r^2 + 4c^2)\sqrt{r^2 + c^2} \tag{3.3}$$

3.1. Heat flow in bodies with nonlinear material properties

In this case the thermal conductivity k depends on the temperature $u(x, y)$ (Katsikadelis and Nerantzaki, 1999b). If we assume that $k = k_0[1 + \beta(u - u_0)/u_0]$, where k_0, β and u_0 are constants, the governing equation is written as

$$k\nabla^2 u + \beta(u_x^2 + u_y^2) = 0 \tag{3.4}$$

Table 1. Temperature in a square plate with temperature dependent conductivity

| Position | | u | | | | |
|----------|-----|--------|-----------|----------|----------|-----------|
| x | y | DRM | Kirchhoff | AEM | | |
| | | | | $M = 25$ | $M = 69$ | $M = 225$ |
| 0.1 | 0.5 | 314.15 | 314.00 | 314.44 | 314.17 | 314.19 |
| 0.3 | 0.5 | 338.34 | 337.82 | 339.23 | 337.76 | 338.83 |
| 0.5 | 0.5 | 358.49 | 358.11 | 359.51 | 358.11 | 359.00 |
| 0.7 | 0.5 | 376.27 | 376.08 | 376.62 | 376.68 | 375.97 |
| 0.9 | 0.5 | 392.43 | 392.36 | 392.24 | 392.40 | 391.93 |

Numerical results for a square plane body with $k_0 = 1, \beta = 3, u_0 = 300$ and unit side length $0 \leq x, y \leq 1$ under the mixed boundary conditions $u(0, y) = 300, u(1, y) = 400, u_n(x, 0) = 0, u_n(x, 1) = 0$ are given in Table 1 as compared with those obtained using the Dual Reciprocity Method and the Kirchhoff's transformation method.

3.2. Determination of a surface with constant Gaussian curvature

A surface that passes through a skew closed space curve and has given the Gaussian curvature K is determined from the following boundary value problem (Katsikadelis and Nerantzaki, 1999b)

$$\begin{aligned} u_{xx}u_{yy} - u_{xy}^2 - K(1 + u_x^2 + u_y^2) &= 0 && \text{in } \Omega \\ u &= \tilde{u} && \text{on } \Gamma \end{aligned} \quad (3.5)$$

where Ω is the domain surrounded by the projection Γ of the curve on the x, y plane. Numerical results for the square domain $0 \leq x, y \leq 5$ with the boundary conditions $u(0, y) = \sqrt{50 - y^2}$, $u(5, y) = \sqrt{25 - y^2}$, $u(x, 0) = \sqrt{50 - x^2}$, $u(x, 5) = \sqrt{25 - x^2}$ and the Gaussian curvature $K = 1/50$ are given in Table 2 as compared with the exact ones.

Table 2. Numerical results for u in Example 3.2

| x | $y = 1.25$ | | $y = 3.75$ | |
|------|------------|-------|------------|-------|
| | AEM | Exact | AEM | Exact |
| 0.25 | 6.92 | 6.95 | 5.94 | 5.98 |
| 0.75 | 6.82 | 6.91 | 5.81 | 5.94 |
| 1.25 | 6.70 | 6.84 | 5.68 | 5.86 |
| 1.75 | 6.56 | 6.73 | 5.55 | 5.73 |
| 2.25 | 6.40 | 6.58 | 5.39 | 5.55 |
| 2.75 | 6.21 | 6.39 | 5.18 | 5.32 |
| 3.25 | 6.01 | 6.15 | 4.91 | 5.03 |
| 3.75 | 5.71 | 5.86 | 4.59 | 4.67 |
| 4.25 | 5.39 | 5.51 | 4.20 | 4.22 |
| 4.75 | 5.03 | 5.08 | 3.68 | 3.65 |

3.3. The problem of minimal surface

This is the problem of determining a surface passing through one or more non-intersecting skew closed space curves and having a minimal area. The physical analog is the surface that a soap bubble assumes when constrained by bounding contours (Plateau's problem). The condition

$$\min A = \int_{\Omega} (1 + u_x^2 + u_y^2) \, dx dy \quad (3.6)$$

requires that the minimal surface $u(x, y)$ is a solution to the following boundary value problem (Katsikadelis and Nerantzaki, 2001)

$$\begin{aligned} (1 + u_y^2)u_{xx} - 2u_xu_yu_{xy} + (1 + u_x^2)u_{yy} &= 0 && \text{in } \Omega \\ u &= \tilde{u} && \text{on } \Gamma \end{aligned} \tag{3.7}$$

3.3.1. *The catenoid*

The minimal surface supported on two concentric circles lying at different levels is known as the *catenoid*. The obtained solution for $R = 5, z = 0$ and $R = 2, z = 3$ is determined and it shown in a graphical form in Fig. 3.

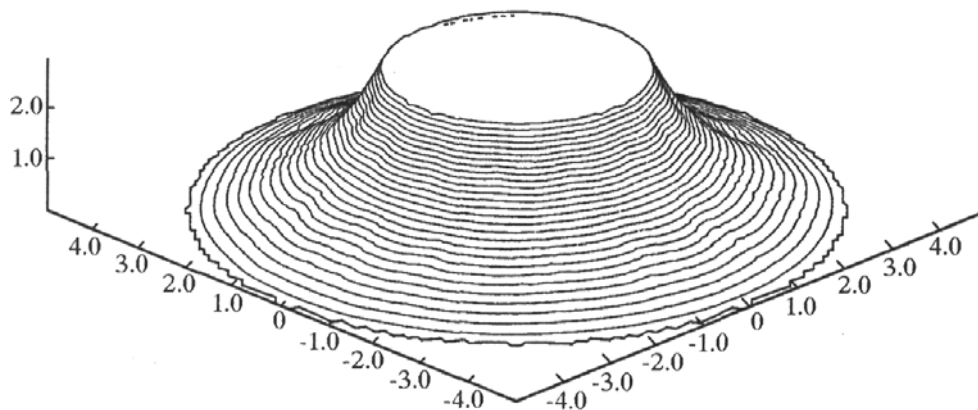


Fig. 3. The catenoid

3.3.2. *Cross shaped membrane*

The surface of a soap bubble that passes through a space curve, which is an intersection of the cylindrical surface $r = 5(\sin^4 \theta + \cos^4 \theta), 0 \leq \theta \leq 2\pi, z \geq 0$, and the sphere $x^2 + y^2 + z^2 = R^2, R = 5$ is determined. The obtained surface is shown in Fig. 5.

3.4. **Large deflections of heterogeneous orthotropic membranes**

Consider a thin flexible initially flat elastic membrane consisting of a heterogeneous orthotropic linearly elastic material occupying the two-dimensional, in general multiply connected, domain Ω in the xy -plane bounded by the $K + 1$ nonintersecting contours $\Gamma_0, \Gamma_1, \dots, \Gamma_K$. The membrane is prestressed either by the imposed displacement \tilde{u}, \tilde{v} or by external forces \tilde{T}_x, \tilde{T}_y acting along the boundary $\Gamma = \bigcup_{i=0}^K \Gamma_i$. Assuming nonlinear kinematic relations, which retain the square of the slopes of the deflection surface, while

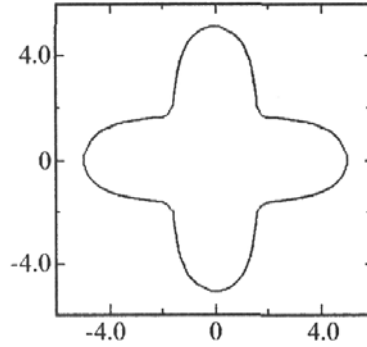


Fig. 4. Plan form of a cross-shaped membrane

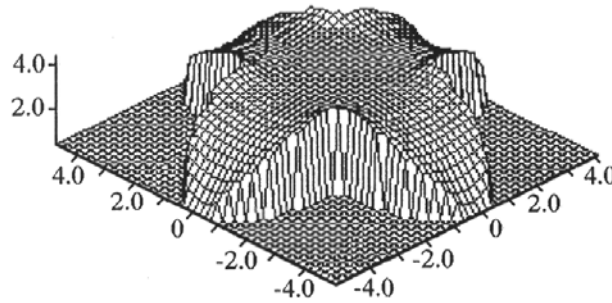


Fig. 5. Cross-shaped membrane

the strain components remain still small compared with the unity, we obtain the following three coupled nonlinear differential equations in terms of the displacements (Katsikadelis and Tsiatas, 2001c)

$$\begin{aligned}
 (C_1 u_{,x} + C v_{,y})_{,x} + (C_{12} u_{,y} + C_{12} v_{,x})_{,y} &= -\left(\frac{C_1}{2} w_{,x}^2 + \frac{C}{2} w_{,y}^2\right)_{,x} - (C_{12} w_{,x} w_{,y})_{,y} \\
 (C_2 v_{,y} + C u_{,x})_{,y} + (C_{12} u_{,y} + C_{12} v_{,x})_{,x} &= -\left(\frac{C_2}{2} w_{,y}^2 + \frac{C}{2} w_{,x}^2\right)_{,y} - (C_{12} w_{,x} w_{,y})_{,x}
 \end{aligned}
 \tag{3.8}$$

$$\begin{aligned}
 &\left[C_1 \left(u_{,x} + \frac{1}{2} w_{,x}^2 \right) + C \left(v_{,y} + \frac{1}{2} w_{,y}^2 \right) \right] w_{,xx} + 2 [C_{12} (u_{,y} + v_{,x} + w_{,x} w_{,y})] w_{,xy} + \\
 &+ \left[C_2 \left(v_{,y} + \frac{1}{2} w_{,y}^2 \right) + C \left(u_{,x} + \frac{1}{2} w_{,x}^2 \right) \right] w_{,yy} = -g
 \end{aligned}$$

subjected to the boundary conditions

$$\begin{aligned}
 T_x &= \tilde{T}_x & \text{or} & & u &= \tilde{u} \\
 T_y &= \tilde{T}_y & \text{or} & & v &= \tilde{v} \\
 T_x w_{,x} + T_y w_{,y} &= \tilde{V} & \text{or} & & w &= \tilde{w}
 \end{aligned}
 \tag{3.9}$$

where $u = u(x, y)$, $v = v(x, y)$ are the in-plane displacement components and $w = w(x, y)$ – the transverse deflection produced when the membrane is subjected to the load $g = g(x, y)$ acting in the direction normal to its plane. The position dependent coefficients $C_1 = C_1(x, y)$, $C_2 = C_2(x, y)$, $C = C(x, y)$ and $C_{12} = C_{12}(x, y)$ characterize the stiffness of the orthotropic membrane and are given as

$$\begin{aligned} C_1 &= \frac{E_1 h}{1 - \nu_1 \nu_2} & C_2 &= \frac{E_2 h}{1 - \nu_1 \nu_2} \\ C &= \frac{E_1 \nu_2 h}{1 - \nu_1 \nu_2} = \frac{E_2 \nu_1 h}{1 - \nu_1 \nu_2} & C_{12} &= Gh \end{aligned} \quad (3.10)$$

in which E_1, E_2 and ν_1, ν_2 are the elastic moduli and the Poisson coefficients in the x and y directions, respectively, constrained by the relation $E_1 \nu_1 = E_2 \nu_2$, and G is the shear modulus.

The analog equations in this case are three uncoupled Poisson's equations, namely

$$\begin{aligned} \nabla^2 u &= b_1(x, y) & \nabla^2 v &= b_2(x, y) \\ \nabla^2 w &= b_3(x, y) \end{aligned} \quad (3.11)$$

The fictitious sources are established using the same procedure with that for one analog equation, and the displacements as well as their derivatives are computed from the integral representations of the solution to the respective Poisson's equations.

3.4.1. Membrane of an arbitrary shape

In this example, a heterogeneous orthotropic membrane of an arbitrary shape is analyzed ($N = 80$, $M = 61$). Its boundary is defined by the curve $r = 5|\sin \theta|^3 + 6|\cos \theta|^3$, $0 \leq \theta \leq 2\pi$. The membrane is prestressed by $u_n = 0.05\text{m}$ in the direction normal to the boundary, while $u_t = 0$ in the tangential direction. The employed data are $h = 0.002\text{m}$, $g = 3\text{kN/m}^2$, $E_1 = E/\sqrt{\lambda}$, $E_2 = E\sqrt{\lambda}$, $\nu_1 = 0.3$, $\nu_2 = \lambda\nu_1$ and $G = E/2(1 + \nu_1\sqrt{\lambda})$ where $E = 110000 + kr^2$, $r = \sqrt{x^2 + y^2}$ and k a constant. The contours of the principle stress resultants N_1 for various values of k and λ are shown in Fig. 6.

3.5. Nonlinear vibrations of membranes

The free and forced vibrations of a homogeneous isotropic membrane is studied. The governing equations result from Eqs (3.8) by setting $C_1 = C_2 = Eh/(1 - \nu^2)$, $C_{12} = E\nu h/(1 - \nu^2)$, and including the inertia force $\rho\ddot{w}$ in the

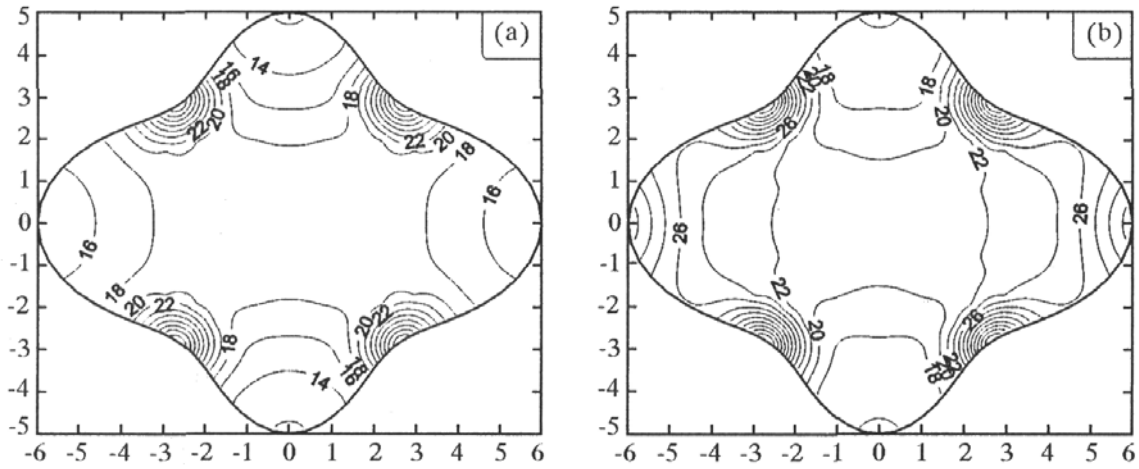


Fig. 6. Contour of N_1 in an orthotropic heterogeneous membrane of an arbitrary shape; (a) $\lambda = 2, k = 0$; (b) $\lambda = 2, k = 5000$

third equation. Thus we have the following initial boundary value problem (Katsikadelis, 2002)

$$\begin{aligned}
 \frac{1-\nu}{2} \nabla^2 u + \frac{1+\nu}{2} (u_{,x} + v_{,y})_{,x} &= -w_{,x} \left(w_{,xx} + \frac{1-\nu}{2} w_{,yy} \right) - \frac{1+\nu}{2} w_{,y} w_{,xy} \\
 \frac{1-\nu}{2} \nabla^2 v + \frac{1+\nu}{2} (u_{,x} + v_{,y})_{,y} &= -w_{,y} \left(w_{,yy} + \frac{1-\nu}{2} w_{,xx} \right) - \frac{1+\nu}{2} w_{,x} w_{,xy} \\
 \rho \ddot{w} - C \left[\left(u_{,x} + \frac{1}{2} w_{,x}^2 \right) + \nu \left(v_{,y} + \frac{1}{2} w_{,y}^2 \right) \right] w_{,xx} - & \\
 -C(1-\nu)(u_{,y} + v_{,x} + w_{,x} w_{,y}) w_{,xy} - & \\
 -C \left[\left(v_{,y} + \frac{1}{2} w_{,y}^2 \right) + \nu \left(u_{,x} + \frac{1}{2} w_{,x}^2 \right) \right] w_{,yy} &= g \quad \text{in } \Omega
 \end{aligned}
 \tag{3.12}$$

$$\left. \begin{aligned}
 T_x &= \tilde{T}_x & \text{or} & \quad u = \tilde{u} \\
 T_y &= \tilde{T}_y & \text{or} & \quad v = \tilde{v} \\
 T_x w_{,x} + T_y w_{,y} &= \tilde{V} & \text{or} & \quad w = \tilde{w}
 \end{aligned} \right\} \quad \text{on } \Gamma$$

$$\left. \begin{aligned}
 w(x, y, 0) &= \tilde{w}_0 \\
 \dot{w}(x, y, 0) &= \dot{\tilde{w}}_0
 \end{aligned} \right\} \quad \text{in } \Omega$$

$$\tag{3.13}$$

3.5.1. Square membrane

A uniformly prestressed ($N_x = N_y = 2.514 \text{ kN/m}, N_{xy} = 0$) square membrane ($0 \leq x, y \leq a$) is studied. The employed data are: $a = 5.0 \text{ m}$,

$h = 0.002$ m, $E = 1.1 \times 10^5$ kN/m², $\nu = 0.3$ and $g_0 = 1.934$ kN/m². The results obtained with $N = 100$ and $M = 49$ are compared with those from the one-term approximate series solution (Ivovich and Pokrovski, 1991), which assumes $w(x, y, t) = w_0(t) \sin(\pi x/a) \sin(\pi y/a)$. In Fig. 7 and Fig. 8 the results for natural vibrations are shown for (i): $w(x, y, 0) = w_0 \sin(\pi x/a) \sin(\pi y/a)$ and $\dot{w}(x, y, 0) = 0$, ($w_0 = 0.446$); (ii): $w(x, y, 0)$ is the deflection surface produced by the static load g_0 and $\dot{w}(x, y, 0) = 0$.

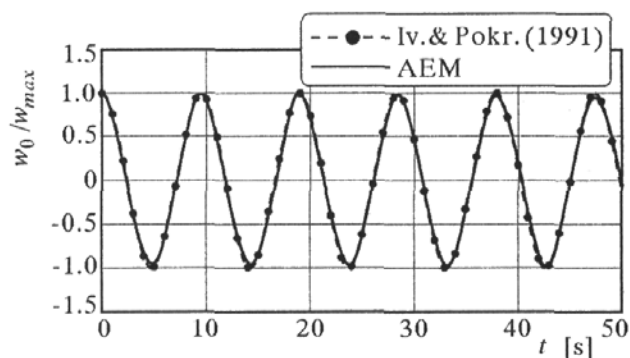


Fig. 7. Central deflection. Case (i)

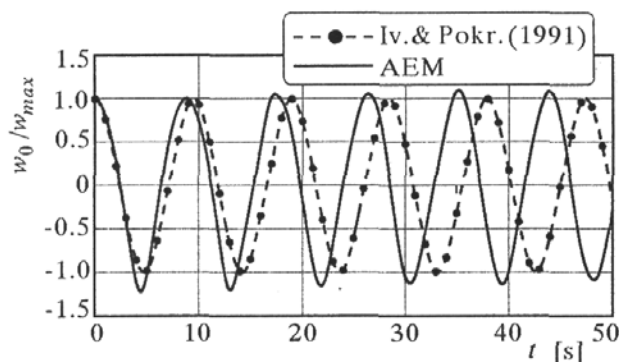


Fig. 8. Central deflection. Case (ii)

Moreover, in Fig. 9, the dependence of the period T (T_0 is the period of the linear vibration) on the maximum amplitude is shown for both cases. It should be noted that the approximate solution gives very good results in case (i). Finally, the forced vibrations have been studied under the so-called "static" load $g = g_0 t/2t_1$ for $0 \leq t \leq t_1$ and $g = g_0/2$ for $t_1 \leq t$, ($t_1 = 10$ s) with zero initial conditions. The response ratio $R(t) = w(0, 0, t)/w_{st}$ of the central deflection is shown in Fig. 10 as compared with that obtained by the one-term approximate solution; w_{st} is the central static deflection obtained by the AEM solution. Apparently, the "static" load produces smaller deflections in

the AEM solution than in the one-term series solution. Therefore, the increase of the period in the AEM solution has been anticipated on the basis of Fig. 9.

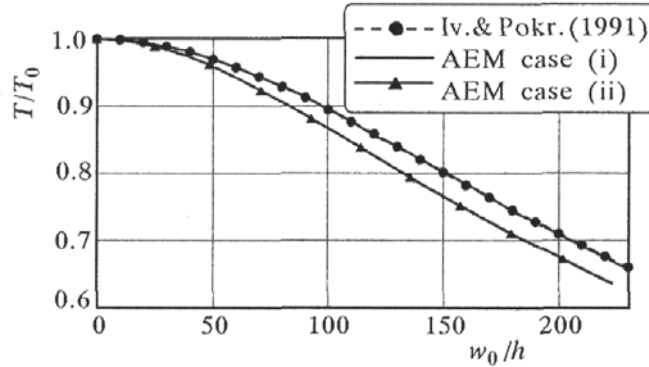


Fig. 9. Period versus maximal central deflection

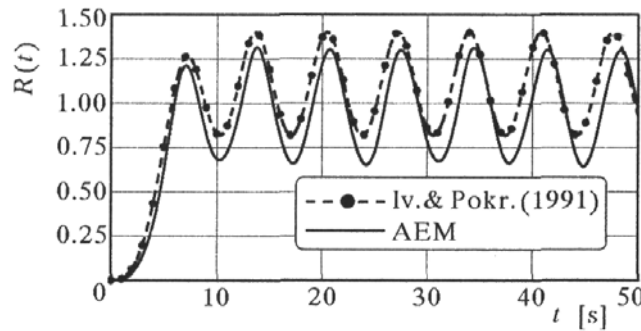


Fig. 10. Response ratio under "static" load

3.6. Plate with variable thickness on nonlinear biparametric elastic foundation

Consider a plate with variable thickness $h = h(\mathbf{x})$, $\mathbf{x} : \{x, y\} \in \Omega$, resting on nonlinear biparametric elastic foundation occupying the two-dimensional multiply connected domain Ω of the x, y -plane, bounded by the $K + 1$ curves $\Gamma_0, \Gamma_1, \Gamma_2, \dots, \Gamma_K$ (Fig. 11). Its response is described by the following boundary value problem (Katsikadelis and Yiotis, 2003)

$$D\nabla^4 w + 2D_{,x}(\nabla^2 w)_{,x} + 2D_{,y}(\nabla^2 w)_{,y} + \nabla^2 D\nabla^2 w - \tag{3.14}$$

$$-(1 - \nu)(D_{,xx} w_{,yy} - 2D_{,xy} w_{,xy} + D_{,yy} w_{,xx}) + p(w, \nabla^2 w) = g(\mathbf{x})$$

$$\alpha_1 w + \alpha_2 V^*(w) = \alpha_3 \quad \beta_1 w_{,n} + \beta_2 M^*(w) = \beta_3 \tag{3.15}$$

where $w(\mathbf{x})$ is the deflection, $g(\mathbf{x})$ is the transverse load, $p(w, \nabla^2 w)$ a nonlinear function of its arguments describing the subgrade reaction and $D = Eh^3/12(1 - \nu^2)$ the variable flexural stiffness of the plate. Moreover, $\alpha_i = \alpha_i(\mathbf{x})$, $\beta_i = \beta_i(\mathbf{x})$, $\mathbf{x} \in \Gamma$, are functions specified on Γ ; $M^*(w)$ and $V^*(w)$ the normal bending moment and the effective shear force on the boundary. The boundary conditions (3.15) are the most general linear boundary conditions for the plate bending problem including also transverse and rotational elastic support. All types of conventional boundary conditions can be derived from (3.15) by specifying appropriately the functions α_i and β_i .

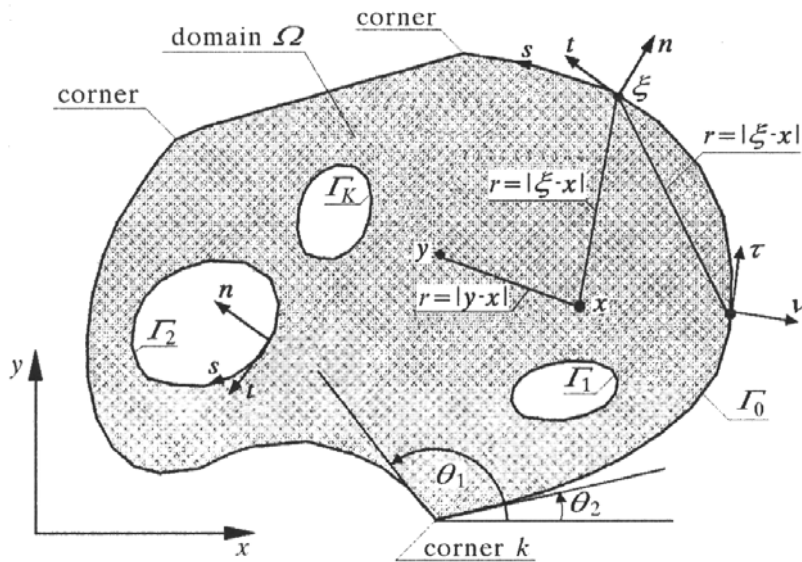


Fig. 11. Plate geometry and notation

Taking into account that the flexural rigidity D is a position dependent function and using boundary curvilinear coordinates n and s , the operators M^*, V^* appearing in Eqs (3.15) are written as

$$M^* = -D \left[\nabla^2 + (\nu - 1) \left(\frac{\partial^2}{\partial s^2} + \kappa \frac{\partial}{\partial n} \right) \right] \tag{3.16}$$

$$V^* = -D \left[\frac{\partial}{\partial n} \nabla^2 - (\nu - 1) \frac{\partial}{\partial s} \left(\frac{\partial^2}{\partial n \partial s} - \kappa \frac{\partial}{\partial s} \right) \right] + \frac{\partial D}{\partial s} (\nu - 1) \left(\frac{\partial^2}{\partial n \partial s} - \kappa \frac{\partial}{\partial s} \right) - \frac{\partial D}{\partial n} \left[\nabla^2 + (\nu - 1) \left(\frac{\partial^2}{\partial s^2} + \kappa \frac{\partial}{\partial n} \right) \right]$$

in which $\kappa = \kappa(s)$ is the curvature of the boundary.

In the case of free or transversely elastically restrained edges, the boundary conditions (3.15) must be supplemented with the corner condition

$$c_{1l}w + c_{2l}[[T^*(w)]]_l = c_{3l} \quad c_{2l} \neq 0 \tag{3.17}$$

where c_{ik} are specified constants at the corner point \mathbf{x}_l and T^* is the operator

$$T^* = D(1 - \nu) \left(\frac{\partial^2}{\partial s \partial n} - \kappa \frac{\partial}{\partial s} \right) \tag{3.18}$$

Thus, $T^*(w)$ is the twisting moment along the boundary and $[[T^*(w)]]_l$ its jump of discontinuity at the corner point \mathbf{x}_l .

It should be emphasized that for the biparametric foundation the free boundary, in contrast to the clamped or simply supported, allows interaction between the deflections of the foundation area under the plate and that of outside it. Therefore the boundary condition (3.15)₁ should be appropriately modified on the following physical considerations (Katsikadelis and Kallivokas, 1988):

- a) The deflection is continuous across the boundary Γ , while its normal derivative is discontinuous.
- b) The bending moment $M^*(w)$ vanishes on Γ .
- c) The jump of the shear force in the shear layer on Γ is equal to the effective shear force of the plate $V^*(w)$ on Γ .

The stress resultants at a point inside Ω are given as

$$\begin{aligned} M_x &= -D(w_{,xx} + \nu w_{,yy}) & M_y &= -D(w_{,yy} + \nu w_{,xx}) \\ M_{xy} &= D(1 - \nu)w_{,xy} \\ Q_x &= -D\nabla^2 w_{,x} - D_{,x}(w_{,xx} + \nu w_{,yy}) - D_y(1 - \nu)w_{,xy} \\ Q_y &= -D\nabla^2 w_{,y} - D_{,y}(w_{,yy} + \nu w_{,xx}) - D_x(1 - \nu)w_{,xy} \end{aligned} \tag{3.19}$$

The analog equation of Eq. (3.14) is

$$\nabla^4 w = b(\mathbf{x}) \tag{3.20}$$

Equation (3.20), indicates that the solution of the original boundary value problem can be obtained as the solution of a linear bending problem for a

plate having unit stiffness and subjected to fictitious load $b = b(\mathbf{x})$ under the given boundary conditions.

The unknown load distribution $b = b(\mathbf{x})$ is established using the direct BEM for thin plates with constant thickness based on the Rayleigh-Green reciprocal identity after modifying it to include the natural boundary quantities, i.e. the normal bending moment and the reaction force along the boundary.

The solution of Eq. (3.20) is written in integral form as

$$\begin{aligned}
 w(\mathbf{x}) = & \int_{\Omega} vb \, d\Omega + \int_{\Gamma} [vV(w) - wV(v) - v_{,n} M(w) + w_{,n} M(v)] \, ds + \\
 & + \sum_{l=1}^L [[vT(w) - wT(v)]_l
 \end{aligned} \tag{3.21}$$

where

$$v = \frac{1}{8\pi} r^2 \ln r \quad r = \|\boldsymbol{\xi} - \mathbf{x}\| \quad \begin{cases} \mathbf{x} \in \Omega \\ \boldsymbol{\xi} \in \Gamma \end{cases} \tag{3.22}$$

is the fundamental solution of the biharmonic equation and

$$\begin{aligned}
 V &= -\left[\frac{\partial}{\partial n} \nabla^2 - (\nu - 1) \frac{\partial}{\partial s} \left(\frac{\partial^2}{\partial n \partial s} - \kappa \frac{\partial}{\partial s} \right) \right] \\
 M &= \frac{1}{D} M^* = -\left[\nabla^2 + (\nu - 1) \left(\frac{\partial^2}{\partial s^2} + \kappa \frac{\partial}{\partial n} \right) \right] \\
 T &= \frac{1}{D} T^* = (1 - \nu) \left(\frac{\partial^2}{\partial s \partial n} - \kappa \frac{\partial}{\partial s} \right)
 \end{aligned} \tag{3.23}$$

are the operators that produce the boundary reactions of the fictitious plate, i.e. the effective shear force, the normal bending moment and the twisting moment along the boundary. Note that

$$V(w) = \frac{1}{D} V^*(w) - (\nu - 1) (\ln D)_{,s} (w_{,sn} - \kappa w_{,s}) - \frac{1}{D} (\ln D)_{,n} M^*(w) \tag{3.24}$$

The fictitious load $b(\mathbf{x})$ for the biharmonic operator is established following a procedure analogous to that for the 2nd order operator. The particular solution corresponding to Eq. (3.3) is obtained from the biharmonic equation

$$\nabla^4 \hat{w}_j = f_j \quad j = 1, 2, \dots, M \tag{3.25}$$

which $f_j = \sqrt{r^2 + c^2}$ yields

$$\begin{aligned}
 \hat{w}_j = & -\frac{1}{12} \ln(c\sqrt{r^2 + c^2} + c^2) c^3 (r^2 + c^2) + \frac{7}{60} c^5 \ln(c\sqrt{r^2 + c^2} + c^2) - \frac{1}{12} c^5 + \\
 & + \frac{1}{12} c^3 r^2 - \frac{7}{60} c^4 \sqrt{r^2 + c^2} + \frac{1}{225} (r^2 + c^2)^{5/2} + \frac{2}{45} c^2 \sqrt{(r^2 + c^2)^3}
 \end{aligned} \tag{3.26}$$

3.6.1. Elliptic simply supported plate with quadratic thickness variation law

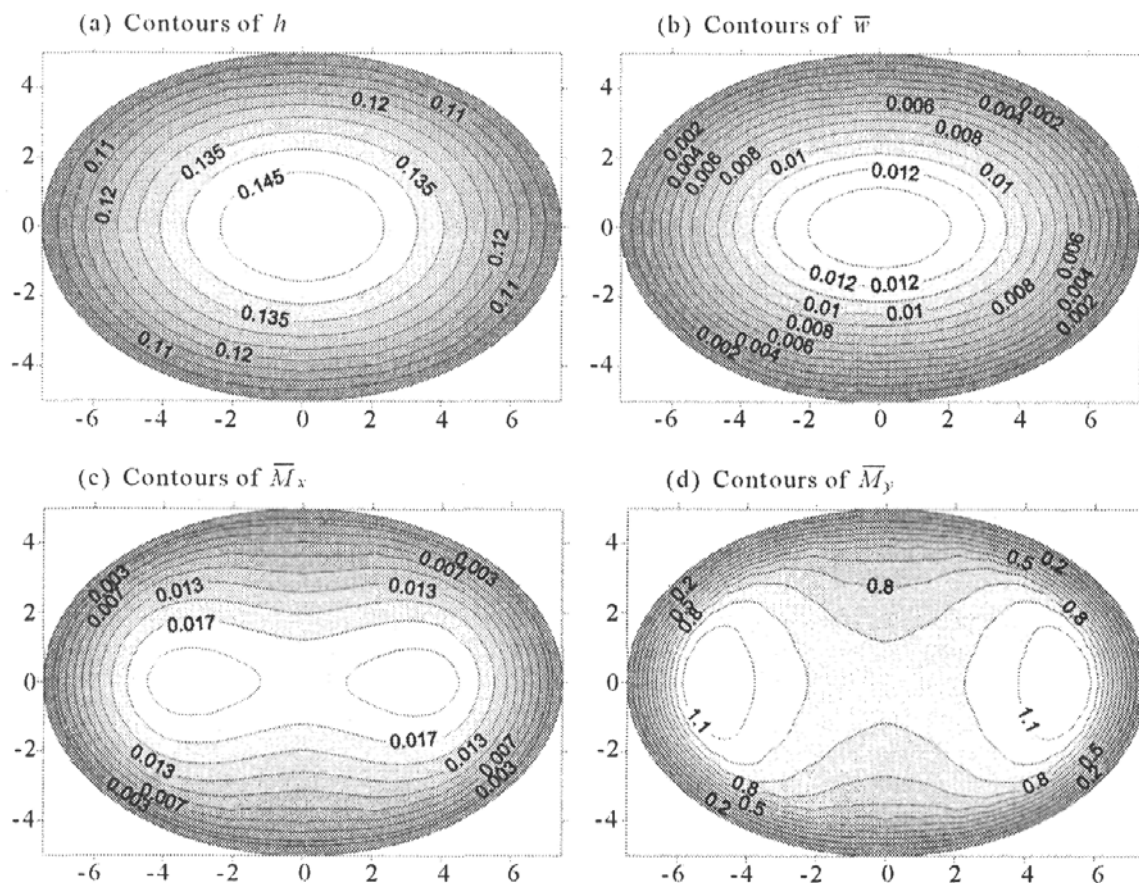


Fig. 12. Simply supported elliptic plate with quadratic thickness variation on nonlinear biparametric elastic foundation

A simply supported elliptic plate resting on nonlinear biparametric elastic foundation, $p = k_0w - k_1w^2 - G\nabla^2w$, has been analyzed. Its boundary is defined by the ellipse $x = a \cos \theta$, $y = b \sin \theta$, $0 \leq \theta \leq 2\pi$. The thickness variation law is specified by the function $h(r) = (h_B - h_0)(r/R)^2 + h_0$, $0 \leq r \leq R$, where h_0 is the plate thickness at the center of the plate and h_B its constant thickness along the boundary; $R = \sqrt{x^2 + y^2}$ is the radial distance from the center of the plate to the boundary. The contours of the plate thickness are shown in Fig. 12a. The curvature of the elliptic boundary is obtained as $\kappa(s) = ab/[a^2 + (b^2 - a^2) \cos^2 \theta]^{3/2}$. The plate is subjected to uniform load $g = g_0$. The numerical results have been obtained for $E = 2.1 \cdot 10^6 \text{ kN/m}^2$, $\nu = 0.3$, $\lambda_0 = 2.11$, $\lambda_1 = 3$, $s = 7$, ($\lambda_i = a/a\sqrt[4]{D_0/k_i}$, $s = a/a\sqrt{D_0/G}$, $i = 0, 1$), $h_0 = 0.15 \text{ m}$, $h_B = 0.10 \text{ m}$, $N = 80$, $M = 85$. The computed deflections $\bar{w} = w/(g_0b^4/D_0)$, bending moments $\bar{M}_x = M_x/g_0b^2$ and the subgrade reaction $\bar{p} = p/g_0$ are presented in Table 3. Moreover, the contours of the

computed deflections $\bar{w} = w/(g_0b^4/D_0)$, bending moments $\bar{M}_x = M_x/g_0b^2$ and $\bar{M}_y = M_y/g_0b^2$ are shown in Fig. 12b,c,d.

Table 3. Deflections $\bar{w} = w/(g_0b^4/D_0)$ and bending moments $\bar{M}_x = M_x/g_0b^2$ at the center of an elliptic simply supported plate with quadratic thickness variation ($\nu = 0.3$) on nonlinear biparametric elastic foundation

| a/b | λ_0, λ_1, s | | h_0/h_B | | |
|-------|--|-------------|-----------|-----------|----------|
| | | | 1.0 | 1.2 | 1.5 |
| 1 | $\lambda_0 = 2.11$ $\lambda_1 = 3$ $s = 7$ | \bar{w} | 0.004384 | 0.004427 | 0.004455 |
| | | \bar{M}_x | 0.012250 | 0.012060 | 0.011880 |
| | | \bar{p} | 0.997900 | 0.984400 | 0.970900 |
| 7.5/5 | $\lambda_0 = 2.11$ $\lambda_1 = 3$ $s = 7$ | \bar{w} | 0.013270 | 0.013590 | 0.013830 |
| | | \bar{M}_x | 0.022110 | 0.020280 | 0.018550 |
| | | \bar{p} | 0.977400 | 0.9557600 | 0.937100 |

4. Conclusions

- As the method is boundary-only, it has all the advantages of the BEM, i.e. the discretization and integration are performed only on the boundary.
- Simple static known fundamental solutions are employed for both static and dynamic problems. They depend only on the order of the differential equation and not specific differential operator which governs the problem under consideration.
- The computer program is the same for both static and dynamic problems and depends only on the order of the differential equation and not specific differential operator which governs the problem under consideration.
- The deflections and the stress resultants are computed at any point using the respective integral representation as mathematical formulas.
- Accurate numerical results for the displacements and the stress resultants are obtained using radial basis functions of multiquadric type.
- The concept of the analog equation in conjunction with radial basis functions approximation of the fictitious sources renders BEM a versatile computational method for solving difficult nonlinear static and dynamic engineering problems for non-homogeneous bodies.

References

1. IVOVICH V.A., POKROVSKI L.N., 1991, *Dynamic Analysis of Suspended Roof Systems*, Chapt. 6 A.A. BALKEMA, Rotterdam
2. KATSIKADELIS J.T., 1994a, A new time step integration scheme for structural dynamics based on the analog equation method, In: *Collection of papers dedicated to Prof. P.S. Theocaris*, ed. A.N. Kounadis, National Technical University of Athens, Athens, 80-100
3. KATSIKADELIS J.T., 1994b, The analog equation method-A powerful BEM-based solution technique for solving linear and nonlinear engineering problems, In: *Boundary Element Method, XVI*, ed. C.A. Brebbia, Computational Mechanics Publications, 167-182
4. KATSIKADELIS J.T., 2001, Finite deformation of elastic cables under 3-D loading, In: *Proc. 4th German-Greek-Polish Symposium on Advances on Mechanics*, Warsaw-Pultusk
5. KATSIKADELIS J.T., 2002, Dynamic analysis of nonlinear membranes by the analog equation method. A boundary-only solution, *Computational Mechanics*, **29**, 170-177
6. KATSIKADELIS J.T., APOSTOLOPOULOS N., 1995, Finite deformation analysis of cables by the analog equation method, In: *Eurosteel'95: Steel Structures*, ed. A.N. Kounadis, BALKEMA, Rotterdam, 355-360
7. KATSIKADELIS J.T., KALLIVOKAS L.F., 1988, Plates on biparametric elastic foundation by BDIE method, *Journal of Engineering Mechanics*, **114**, 5, 847-875
8. KATSIKADELIS J.T., NERANTZAKI M.S., 1999a, Solving equationless problems from boundary only data, In: *Proc. of the European Conference on Computational Mechanics*, Munich, Germany, 818
9. KATSIKADELIS J.T., NERANTZAKI M.S., 1999b, The boundary element method for nonlinear problems, *Engineering Analysis with Boundary Elements*, **23**, 365-373
10. KATSIKADELIS J.T., NERANTZAKI M.S., 2001, A boundary element solution to the soap bubble problem, *Computational Mechanics*, **27**, 2, 154-159
11. KATSIKADELIS J.T., NERANTZAKI M.S., TSIATAS G.C., 2001c, The analog equation method for large deflection analysis of membranes. A boundary-only solution, *Computational Mechanics*, **27**, 6, 513-523
12. KATSIKADELIS J.T., TSIATAS G.C., 2001a, Large deflection analysis of beams with variable stiffness. An analog equation solution, In: *Proc. of the 6th National Congress on Mechanics*, Thessaloniki, Greece, I, 172-177

13. KATSIKADELIS J.T., TSIATAS G.C., 2001b, Nonlinear dynamic analysis of heterogeneous orthotropic membranes, In: *Boundary Elements*, **XXIII**, eds. D.E. Beskos, C.A. Brebbia, Katsikadelis J.T. and G. Manolis, WITpress, Southampton, 139-148
14. KATSIKADELIS J.T., TSIATAS G.C., 2001c, The analog equation method for large deflection analysis of heterogeneous orthotropic membranes. A boundary-only solution, *Engineering Analysis with Boundary Elements*, **25**, 8, 655-667
15. KATSIKADELIS J.T., YIOTIS A.J., 2003, The BEM for plates of variable thickness on nonlinear biparametric elastic foundation: An analog equation solution, *Journal of Engineering Mathematics*, (to appear)
16. NERANTZAKI M.S., KATSIKADELIS J.T., 1998, Solving inverse problems by use of the AEM, In: *Inverse Problems in Engineering Mechanics*, eds. M. Tanaka and G. Dulikravich, Elsevier, Tokyo, 335-340
17. PARTRIDGE P.W., BREBBIA C.A., WROBEL L.C., 1992, *The Dual Reciprocity Boundary Element Method*, Computational Mechanics Publications, Southampton
18. YIOTIS A.J., KATSIKADELIS J.T., 2001, The boundary element method for nonlinear analysis of shells, In: *Proc. 4th German-Greek-Polish Symposium on Advances on Mechanics*, Warsaw-Pultusk

Metoda analogowych wyłącznie-brzegowych równań całkowych w zagadnieniach statyki i dynamiki ciał uogólnionych

Streszczenie

W pracy przedstawiono metodę równań analogowych (AEM), metodę wyłącznie brzegową, do rozwiązywania problemów statyki i dynamiki w mechanice ośrodka ciągłego. W rozważaniach uwzględniono ciała uogólnione, tzn. obiekty, których właściwości mogą zależeć od położenia i prędkości, a ich odpowiedź jest nieliniowa. Nieliniowość może wynikać z równań konstytutywnych (nieliniowość materiałowa) lub być następstwem dużych przemieszczeń (nieliniowość geometryczna). Sednem prezentowanej metody jest zamiana nieliniowych i sprzężonych cząstkowych równań różniczkowych o zmiennych współczynnikach, decydujących o odpowiedzi obiektu, układem ekwiwalentnych zlinearyzowanych i rozprzężonych równań z fikcyjną funkcją wejścia. Funkcja ta określana jest za pomocą metody elementów brzegowych, a rozwiązanie pierwotnego problemu jest otrzymywane na podstawie całkowitej reprezentacji rozwiązania problemu zastępczego. W celu demonstracji efektywności i dokładności metody AEM zamieszczono szereg różnych przykładów z dziedziny statyki i dynamiki, które rozwiązano tą metodą.